Effects of Taheri Consciousness Fields on Concrete (ASR)

Bahareh Kazazi[1*], Mohammad Ali Taheri[2]

The First Journal in T-Consciousness Research
Journal of CosmoIntel
50

1. Civil Engineering, CEO of Hoobe Construction Company, Tehran, Iran.

2. Sciencefact R&D Department, Cosmointel Inc. Research Center, Ontario, Canada.

* Corresponding author:

Bahareh Kazazi
Civil Engineering, CEO of Hoobe Construction Company, Tehran, Iran.

Email: baharkazazi@gmail.com

ABSTRACT

The Alkali-silica reaction of concrete is known as one of the destructive reactions. There are many studies in this area. Taheri Consciousness Fields (TCFs) were founded and introduced by Mohammad Ali Taheri as new Fields. These Fields are neither matter nor energy, therefore, do not possess a quantity, but they have direct effects on both matter and energy. In other words, although TCFs cannot be directly measured, we can investigate their effects indirectly through various controlled experiments. In this study, cement mortar samples were examined by using the ASTM C1260 standard and under the effect of a type of TCF known as TCF(H). Additional experiments, aggregate petrography, L.O.I (Loss on Ignition), SEM (Scanning electron microscopy), XRD (X-ray Diffraction), XRF (X-Ray Fluorescence), FT-IR (Fourier-transform infrared spectroscopy) were performed to further investigate the effect of TCF(H). It was found that the TCF (H) was able to reduce the expansion and improve the cement mortar function by up to 10% (average ~ 7% P-value= 0.008) and make observable changes in chemical and elemental compositions.

Keywords: ASR concrete silica alkali reaction, Taheri Consciousness Fields, T-Consciousness, Intelligence

INTRODUCTION

Concrete is one of the most widely used building materials in the world. Aggregates make up about 60 to 70% of the concrete volume. Aggregates have a great impact on the physical and chemical properties of concrete. In principle, their properties affect the performance, reliability, and behavior of concrete. One of the major effects of aggregate on concrete is the chemical reactions of aggregate with cement inside concrete [1]. One of the most important reactions is the alkaline reaction of aggregate, which is known as concrete cancer. The main cause of this reaction is the chemical composition of the aggregate, which is surrounded by the hydrated cement paste and thus internal pressures are created, which eventually cause expansion and cracking, and disintegration of the concrete. It has also been observed that some of the gel leaks out with the water and settles in cracks that have been already formed due to the swelling of the aggregates, causing other destructive agents to penetrate.

The alkaline reaction is especially important in dam construction projects because the cost of repairing a dam is very high. In previous years, in Canada, after 20 years, the cost of repairing a dam was more than the initial cost of construction [2]. Therefore, different countries put identification, prevention, and repair methods on their agenda. Of course, it should be noted that the best method is to study the history of the aggregate performance during 15 years of operation, and it is necessary to study it beyond just the physical characteristics and include the components and functional environment of concrete. In this way, a comprehensive solution may be suggested. In the absence of such conditions, the design of an alternative test to simulate aggregate behavior and prevention is necessary [3]. To find the proposed solution, it is necessary to know how the aggregate functions in concrete. In general, aggregates cause alkaline reactions in two ways:

A. Alkaline carbonate reaction

The cause of this reaction is the alkali in cement and a group of dolomitic lime aggregates that cause cracks in wet conditions [1-4]. and is less studied due to its rarity.

B. Alkaline silica reaction (ASR)

This reaction was first known in California in 1930, [5] the Alkaline-silica reaction (ASR) is a chemical process in which OH^- ions present in the solution of the concrete pores are combined with the weakly crystalline and amorphous silica in the aggregates in concrete; and ASR compounds are then produced. The presence of water and constant swelling leads to an increase in stress and fracture of the concrete. When the internal stress reaches more than the tensile strength of the concrete, cracks are generated [6].

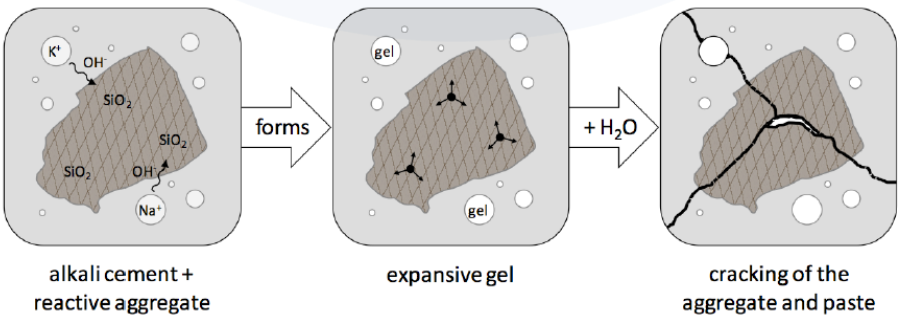

Figure 1 - Schematic drawing of the concrete cracking process by alkali-silica reaction

In general, the effective factors in this reaction are the presence of unstable silicas, and aluminosilicates, [7-8] sufficient alkaline compounds in the water inside the concrete pores, and the presence of moisture. Research has been done regarding the details and the extent of the effect of each of these factors in performing the reaction. The latest research has examined their effect, particularly water, on the size and structure, and growth of gels at the nanoscale [9].

In addition to the cases that are required for gel formation, the rate of expansion of the reaction depends on factors such as the number of ions in concrete, type of cement, pozzolans used, conditions of the performance environment, sources, and ion accumulation sites along with ambient humidity and ambient temperature [10-12]. The main subject of this research, considering the extent of this destruction, is further studied in this section.

Methods of Control and prevention of concrete cancer

The most well-known methods of controlling or preventing alkaline silica reaction

Given the importance of this destructive response, engineers from the beginning thought of solutions to control and repair structures, many of which have been used in industry for years and are constantly being improved. One of the most well-known methods is the use of gel-controlling pozzolans, the most famous of which are:

Use of low alkali cement and the addition of minerals and chemicals such as fly ash [13], Silica fume [14-15], Slag of smelting iron and copper furnaces [16], and use of nano-silicates silica powder [17], Lithium salts [18-19], and even environmentally friendly methods such as the use of rubber fragments [20] or rice husk [21]. In Iran, zeolite has been also used for many years due to its availability in the structure of dams [22-23].

The extent of application of all the above methods depends on parameters such as the type of cement and environmental conditions on the one hand and the study of other mechanical and chemical properties of concrete on the other hand. Therefore, all methods have limitations and a distinct range of effects. According to the recommendation of research institutes, the best method is still to identify destructive aggregates and prevent their use or control the amount of alkali in cement. A good solution for this problem is a method of control that is simple, comprehensive, and independent of other constraints [24].

Taheri Consciousness Fields

The nature of consciousness and its place in science has received much attention in the current century. Many philosophical and scientific theories have been proposed in this area. In the1980s, Mohammad Ali Taheri introduced novel fields with a non-material/non-energetic nature named Taheri Consciousness Fields (TCFs). In this perspective, T-Consciousness is one of the three existing elements of the universe apart from matter and energy. According to this theory, there are various TCFs with different functions, which are the subcategories of a networked universal internet called the Cosmic Consciousness Network (CCN). The major difference between the theory of TCFs and other theoretical concepts about consciousness is related to the practical application of the TCFs. TCFs can be applied to all living and non-living creatures, including plants, animals, microorganisms, materials, etc.

Mohammad Ali Taheri, the founder of Er-

fan Keyhani Halqeh, a school of thought, introduced a new science in 2020 as a branch of this school. He coined the term Sciencefact for this new science because it utilizes scientific investigations to prove the existence of T-Consciousness as an irrefutable phenomenon and a fact. Although science focuses solely on the study of matter and energy and Sciencefact, by contrast, explores the effects of the [non-material/ non-energetic] TCFs, Sciencefact has provided a common ground between the two by conducting reproducible laboratory experiments in various scientific fields, and it has used the scientific approach in proving TCFs.

The influence of the TCFs begins with the Connection between CCN as the Whole Taheri Consciousness of the universe and the subjects of study as a part. This Connection called "Ettesal" is established by a certified and trained individual who has been entrusted with the TCFs. The human mind has an intermediary role (Announcer) which plays a part by fleeting attention to the subject of study and then the main achievement obtained as a result of the effects of the TCFs. These Fields cannot be directly measured by science, but it is possible to investigate their effects on various subjects through reproducible laboratory experiments.

The research methodology in the study of T-Consciousness has been founded on the process of Assumption, Argument, and Proof, in which the basic Assumption is: The Cosmos was formed by a third element called T-Consciousness that is different from matter and energy.

The Argument: The existence of TCFs can be demonstrated by its effects on matter and energy (e.g., humans, animals, plants, microorganisms, cells, materials, etc.)

The Proof: is the scientific verification of the effects of TCFs on matter and energy (according to the Argument) through various reproducible scientific experiments.

Accordingly, to investigate and verify the existence, effects, and mechanisms of TCFs, the following five research phases (Phases 0 through 4), and the aims of each phase are outlined below.

Phase-0 studies aim to prove the existence of TCFs by observing their effects. The nature of T-Consciousness and what it is will not be addressed in this phase. Phase-1 explores the varied effects of different TCFs. Phase-2 examines the reason behind the varied effects of these fields. Phase-3 investigates the mechanism of TCFs effects on matter and energy. Finally, Phase-4 draws significant conclusions, particularly with regard to the mind and memory of matter and their relation to the T-Consciousness, etc. [25-28]

Materials and Methods

ASTM C 1260

There are different methods for testing the reactivity of aggregates, and in this research standard ASTM C 1260 is the basis of the work [29]. On the other hand, due to the novelty of the knowledge of the CF(H), from each mold that included 4 samples, one sample was selected for the following experiments: Group XI No. 3- Group XII No. 4- Group XIII No. 4- Control Group No. 4. From now on each sample briefly introduces its group and is named by the same group name and is examined for the following tests.

Petrography

The samples and the rock and mortar sections were examined in terms of mineralogy; the shape and form of silica crystals were examined by petrographic imaging.

SEM (Scanning electron microscopy)

Examination of SEM photography and prepa-

ration of images and investigation of the construction and the presence of basic elements.

L.O.I (Loss on Ignition)

Doing L.O.I test to reduce the weight of the sample due to heat.

XRF (X-Ray Fluorescence)

A quantitative and qualitative investigation of oxides of XRF samples.

XRD (X-ray Diffraction)

crystallography study; investigation and identification of crystalline phases and changes in the crystalline structure.

FT- IR (Fourier-transform infrared spectroscopy)

Infrared examination of FT- IR

Methodology of the ASTM C 1260 test

Aggregate used: In order to better investigate the effects of the CF(H), the aggregates were selected from a Kish Island rock mine in Iran, which have high reactivity.

Method: The test was performed according to the ASTM C1260 standard by preparing 4 series, which according to the standard, each series included 4 prism samples. This method was accelerated and strict.

Cement: The Portland cement used for all samples was type II cement from one bag. Since the samples were exposed to NaOH, the number of alkalis in the cement was not a significant factor in expansion.

First, all aggregates were graded according to the requirements of Table1.

Table 1 . Requirements for the grading of the aggregate

Sieves Size (mm)		Weight Percentage
Passed	Remained	
4.75	2.36	10
2.36	1.18	25
1.18	0.600	25
0.600	0.300	25
0.300	0.150	15

Then four molds of each series including 4 standard samples were prepared for each aggregate and cement composition.

Mortar components ratio

The ratio of dry materials for the mortar test was one part of cement to 2.25 parts of aggregate by weight, and the ratio of water to cement was equal to 0.47.

Mixing

Mixing of mortars was performed in accordance with the requirements of the ASTM C305 standard method.

Molding the samples

Immediately after making the mortar, the samples were molded.

Application of Taheri Consciousness Fields

One of the introduced TCFs is called the Consciousness Bond Field and was applied to the samples according to the protocols regulated by the COSMOintel research center (www.COSMOintel.com). A request for Connection to the CCN to utilize TCFs can be placed through the COSMOintel website in the “Assign An-

nouncement" section. This access is available for everyone at no cost. In order to study and experience this Connection, the researchers can register on the website at any time in order to report the experiment to the COSMOintel research center. Certain details of the experiment must be provided to the center; for example, the characteristics or number and name of samples and controls must be specified. This entire experiment was carried out as a double-blind method where lab technicians were completely unaware of the TCFs.

Storage and measurement of samples

Initial storage and reading

Samples were placed in a wet chamber immediately after molding. They were removed from the mold after 24 hours and the initial reading was performed with an accuracy of 0.002 mm. The samples made with one type of aggregate were placed in a sealed chamber that had enough water to drown the samples, and the chamber was placed in an oven at a temperature of 80 ° C ±2 for 24 hours.

Zero base reading

After 24 hours, each of the chambers was removed from the oven in turn, and then the base reading of each of the prisms was done immediately after drying their surfaces, and then they were returned to the chamber, then all samples made from the aggregates were placed in a chamber with a sufficient amount of normal NaOH at a temperature of 80 ° C ±2 so that the samples were completely drowned and the chamber was sealed and returned to the oven.

Subsequent reading and storage

The change in length of the samples was read periodically for 14 days after the baseline reading.

Calculation Method

The difference between base reading (zero) and reading in each time period of the samples was calculated and the expansion of the samples for each period was recorded. The average expansion of four samples for each cement and aggregate composition was reported to be approximately 0.01% of the read periods.

Results and Discussion

Examination of the results in Table 2 shows an average reduction of the rate of expansion of 0.6.6% was observed in the samples under the TCF (H).

Table 2 . The average expansion rate of each series, which is itself an average of the 4 samples, during 16 days

Days	Sand Expansion			
	XI	XII	XIII	Control
2	0.00	0.00	0.00	0.00
9	0.48	0.48	0.43	0.48
14	0.60	0.60	0.56	0.63
16	0.64	0.63	0.60	0.67

Table 3 . Expansion rate of 4 internal samples in each series, at 16 days compared to the control

Name	Sand Expansion			
	XI	XII	XIII	Control
Sample No.1	0.622	0.625	0.614	0.673
Sample No.2	0.614	0.626	0.579	0.671
Sample No.3	0.654	0.635	0.592	0.658
Sample No.4	0.669	0.621	0.606	0.661
The Average percentage of 16-day expansion	**0.64**	**0.63**	**0.6**	**0.67**
Percentage of Change Compared to control at 16 days old	**-4.5%**	**-6%**	**-10.5%**	-------

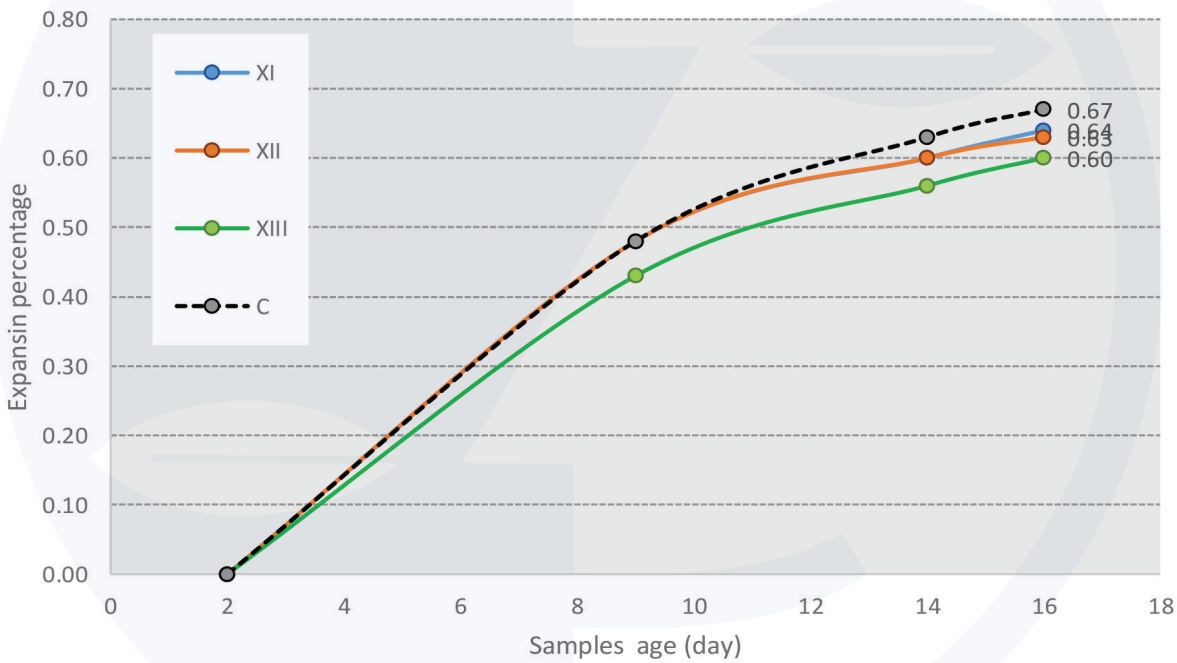

Figure 2 - Comparison of the expansion percentage of samples

Aggregate petrography

Petrography or descriptive petrology is a branch of petrology that discusses the naming, classification, construction, and texture of rock collections. Rocks are heterogeneous natural objects that result from the accumulation of one or more minerals. Usually, in most rocks, the constituent minerals are in balance with each other. The thermodynamic conditions governing the rocks limit the possibility of the presence of minerals together, so it is possible to identify, classify and name the rocks by studying the twin minerals and how they relate to each other in petrography [30].

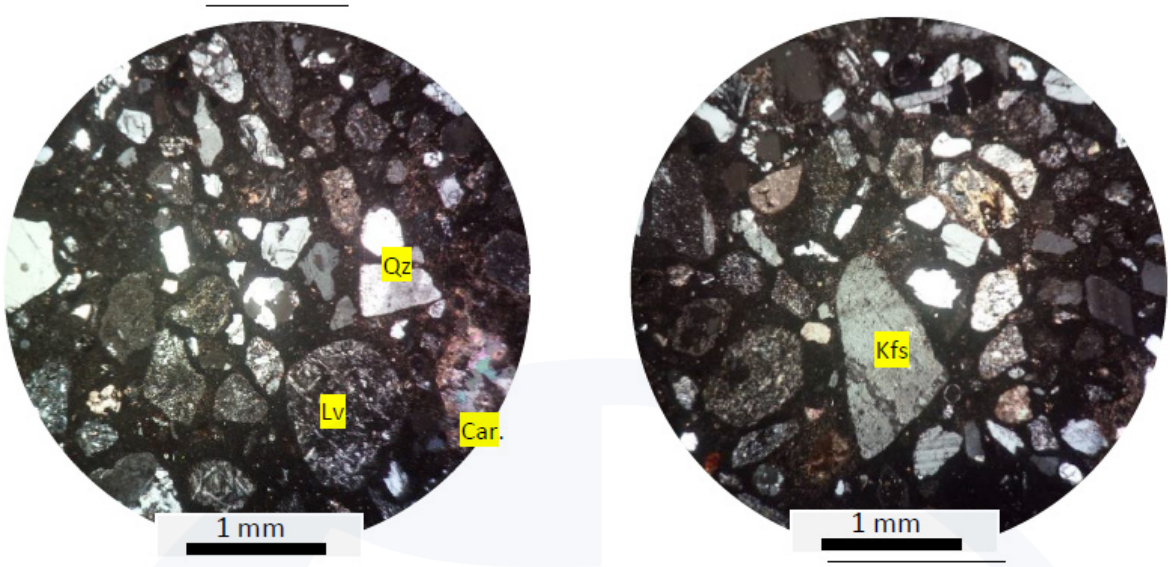

Figure 3 - The Control Sample

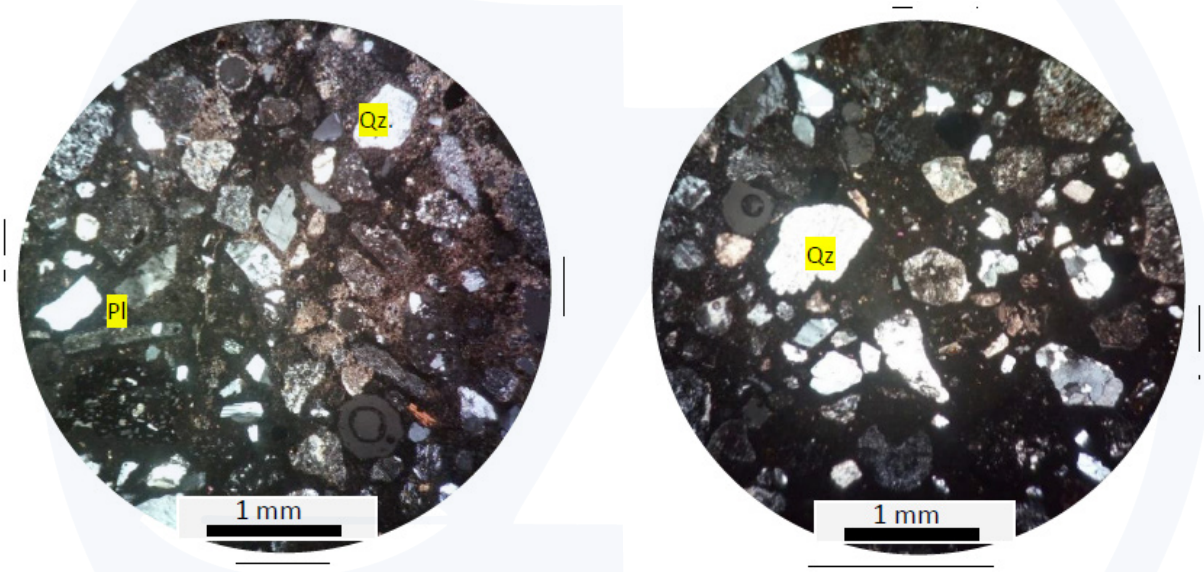

Figure 4 - Sample XI

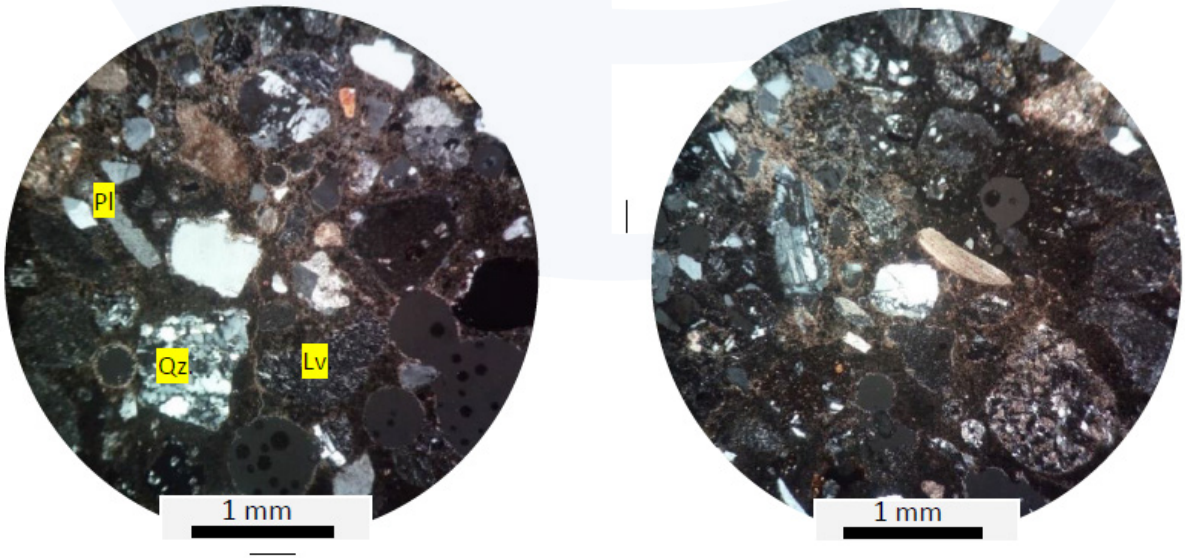

Figure 5 - Sample XII

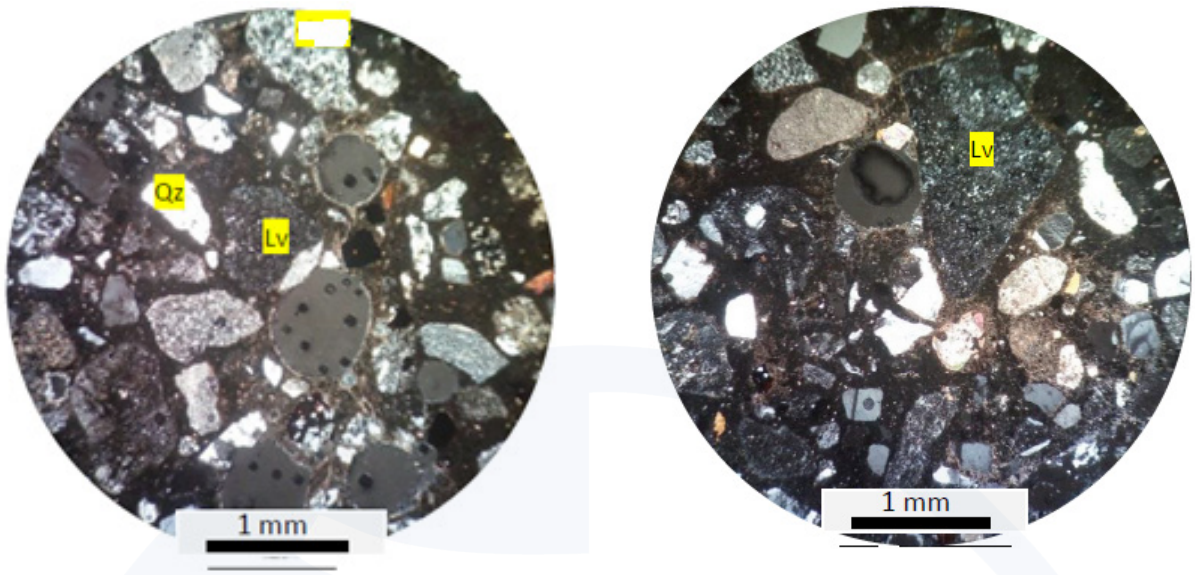

Figure 6- Sample XIII

The identified grains are igneous, sedimentary, and single minerals. The main minerals of the samples are quartz, plagioclases, and potassium feldspar. Igneous components are mainly intermediate to Mafic in composition. Their constituent minerals are plagioclase and pyroxene and are in the form of Photo Cryst in the microcrystalline to glass background. Sedimentary parts are mainly chert, quartz, sandstone, and conglomerate grains as well as carbon parts. Some grains, which are mostly clearer in the samples under the TCF (H), have good roundness, but most of the ones that are more evident in the control sample are more angular. Since the aggregates are freely selected and graded, and according to the full description of how this reaction appears, one of the events is the appearance changes of siliceous minerals. Igneous grains are mainly alteration, and their main minerals are feldspar and quartz minerals. The background of igneous minerals has been completely altered to chlorite. Most of these minerals are quartz and feldspar. Grains' dimensions vary from 100 micrometers to larger than 2 millimeters. The cement background between the grains is completely microcrystalline and covers the space between the grains.

SEM (Scanning Electron Microscopy)

After measuring the expansion rate, the samples were examined by SEM scanning electron microscope, and determination of the chemical composition by point and bulk analysis as an element from different sections.

As it can be seen in figure 8, the apparent difference in the photos is quite obvious. The crystals formed in the control sample are clear and it can be noted that gels are formed around the aggregate. The spaces around the aggregate in the samples under the TCF(H) have a better connection with cement, and less empty and dark space is seen.

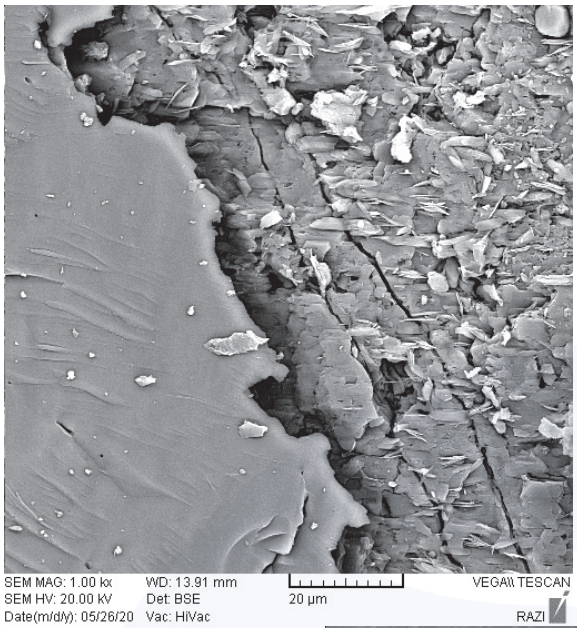

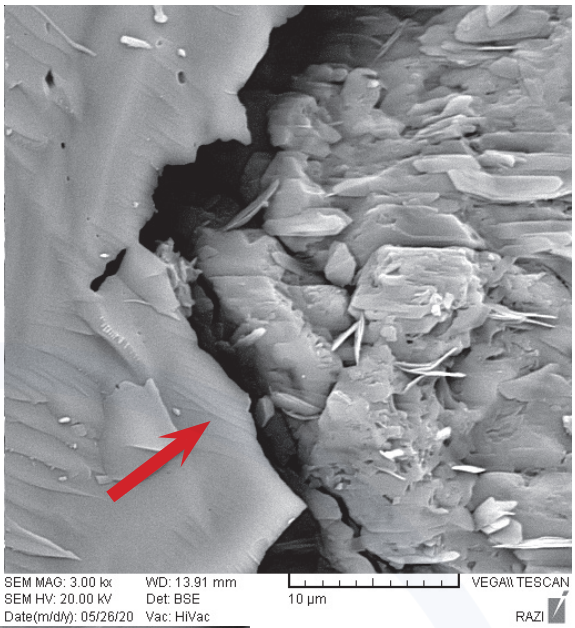

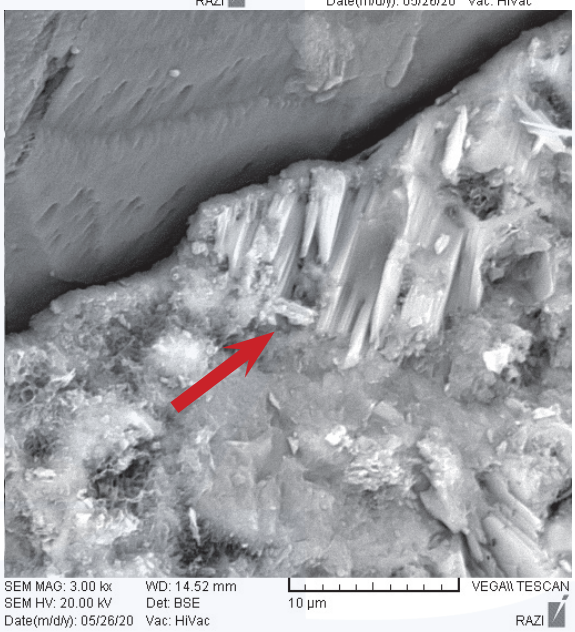

Spectra: SHAHED

Element	Series	unn. C [wt.-%]	norm. C [wt.-%]	Atom. C [at.-%]
Carbon	K series	1.12	1.24	2.13
Oxygen	K series	46.21	51.10	66.30
Sodium	K series	1.79	1.99	1.79
Magnesium	K series	0.41	0.46	0.39
Aluminium	K series	3.09	3.42	2.63
Silicon	K series	21.37	23.63	17.47
Calcium	K series	15.63	17.29	8.95
Iron	K series	0.80	0.88	0.33
	Total:	90.4 %		

Figure 7 - Control sample at the gel formation place, around the aggregates, and weight percentage and atomic number percentage of the elements present in this sample

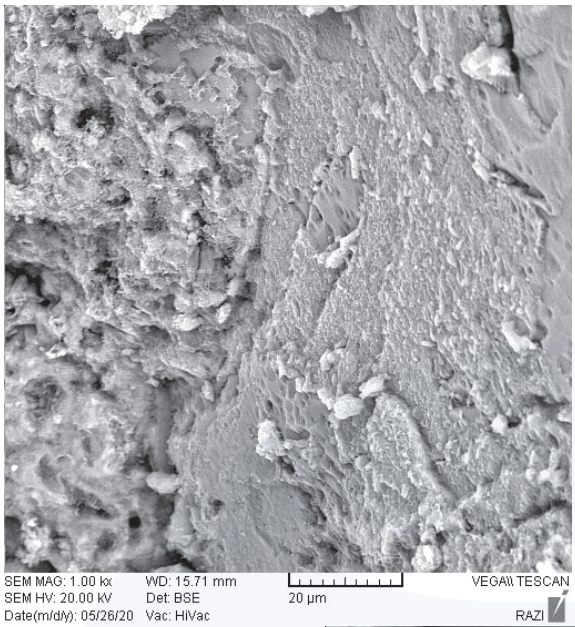

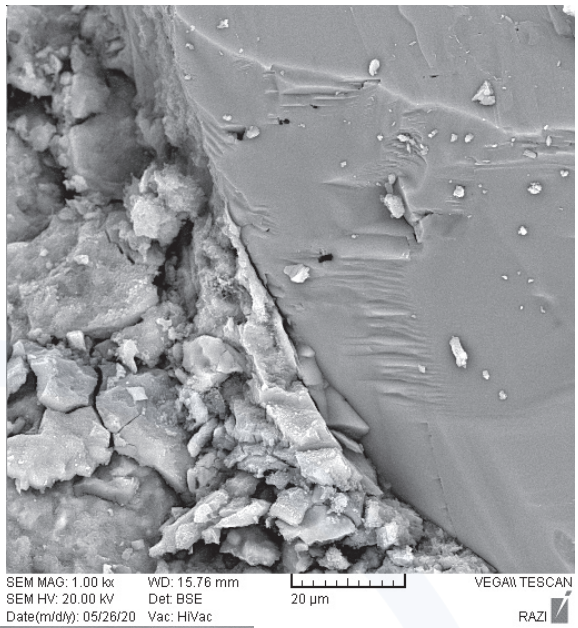

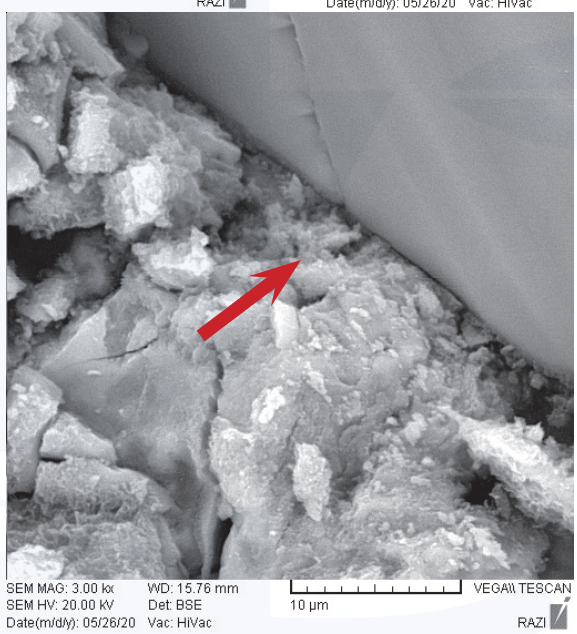

Spectra: SAMPLE 1

Element	Series	unn. C [wt.-%]	norm. C [wt.-%]	Atom. C [at.-%]
Carbon	K series	2.18	2.44	4.50
Oxygen	K series	39.46	44.12	61.12
Sodium	K series	1.00	1.12	1.08
Magnesium	K series	0.65	0.73	0.67
Aluminium	K series	2.32	2.59	2.13
Silicon	K series	14.05	15.71	12.40
Potassium	K series	0.76	0.84	0.48
Calcium	K series	27.05	30.24	16.72
Titanium	K series	0.50	0.56	0.26
Iron	K series	1.47	1.64	0.65
	Total:	89.4 %		

Figure 8 - Sample XI at the gel formation place, around the aggregate, and weight percentage and atomic number percentage of the elements present in this sample

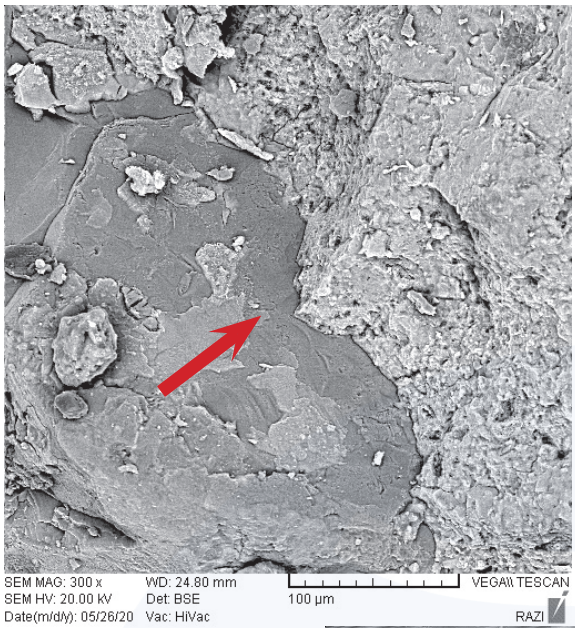

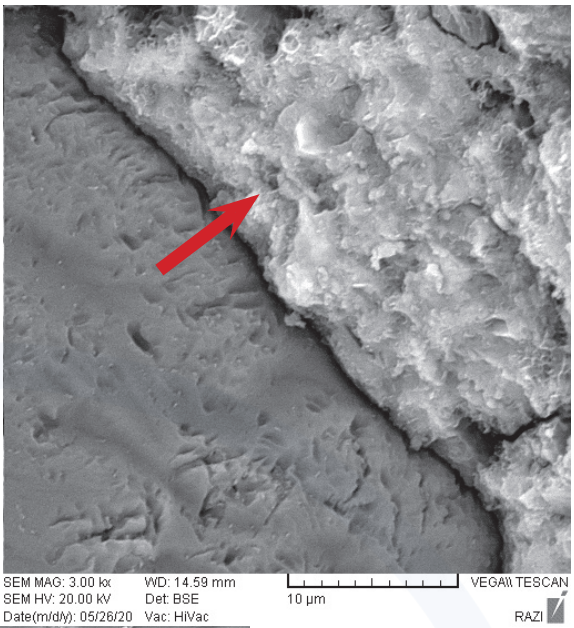

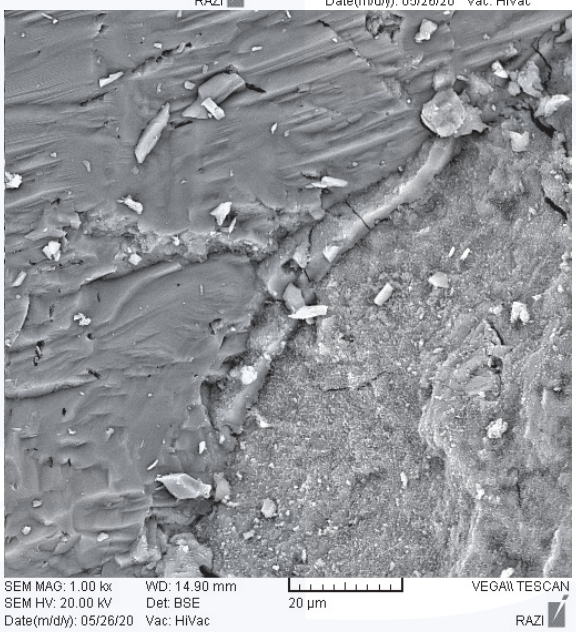

Spectra: SAMPLE 2

Element	Series	unn. C [wt.-%]	norm. C [wt.-%]	Atom. C [at.-%]
Carbon	K series	3.75	4.66	7.95
Oxygen	K series	40.15	49.93	63.95
Sodium	K series	1.57	1.96	1.74
Magnesium	K series	0.54	0.67	0.56
Aluminium	K series	2.07	2.57	1.96
Silicon	K series	12.96	16.12	11.76
Potassium	K series	0.73	0.91	0.48
Calcium	K series	17.23	21.43	10.96
Iron	K series	1.41	1.76	0.64
	Total:	80.4 %		

Figure 9 - Sample XII at the gel formation place, around the aggregate, and weight percentage and atomic number percentage of the elements present in this sample

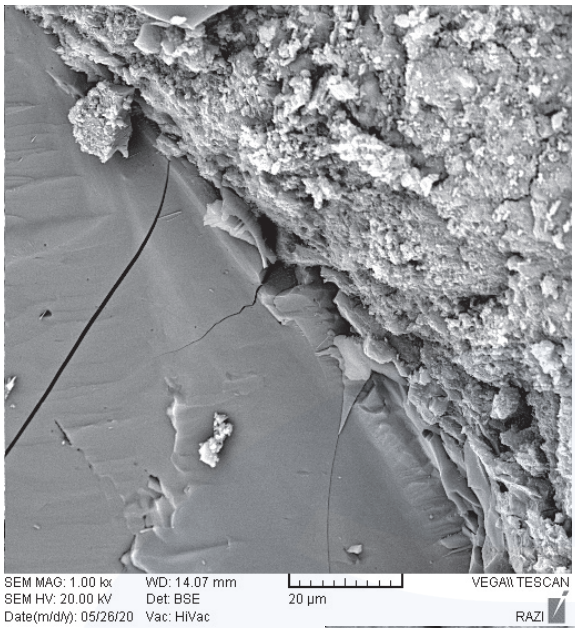

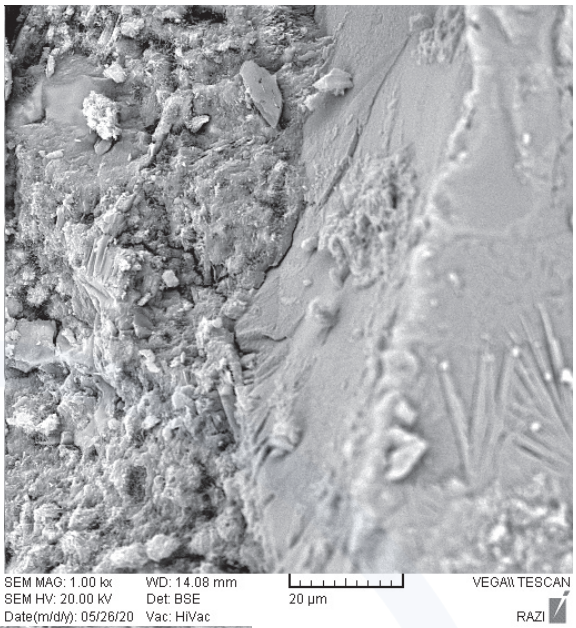

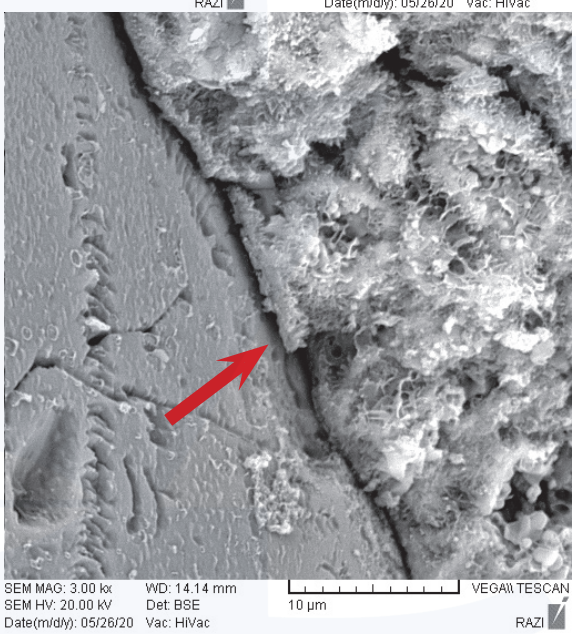

Spectra: SAMPLE 3

Element	Series	unn. C [wt.-%]	norm. C [wt.-%]	Atom. C [at.-%]
Carbon	K series	2.43	2.81	5.07
Oxygen	K series	39.51	45.79	61.97
Sodium	K series	1.48	1.72	1.62
Magnesium	K series	0.52	0.60	0.54
Aluminium	K series	2.55	2.96	2.37
Silicon	K series	13.98	16.21	12.49
Potassium	K series	1.14	1.32	0.73
Calcium	K series	23.37	27.08	14.63
Iron	K series	1.31	1.51	0.59
	Total:	86.3 %		

Figure 10 - Sample XIII in the gel formation place, around the aggregate, and weight percentage and atomic number percentage of the elements present in this sample

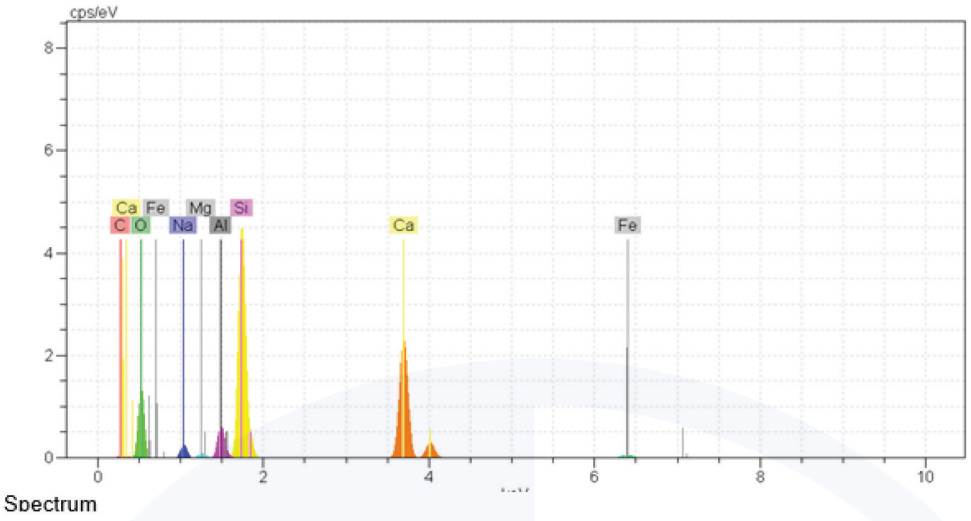

Figure 11 - Identification and abundance of the elements present in the control sample

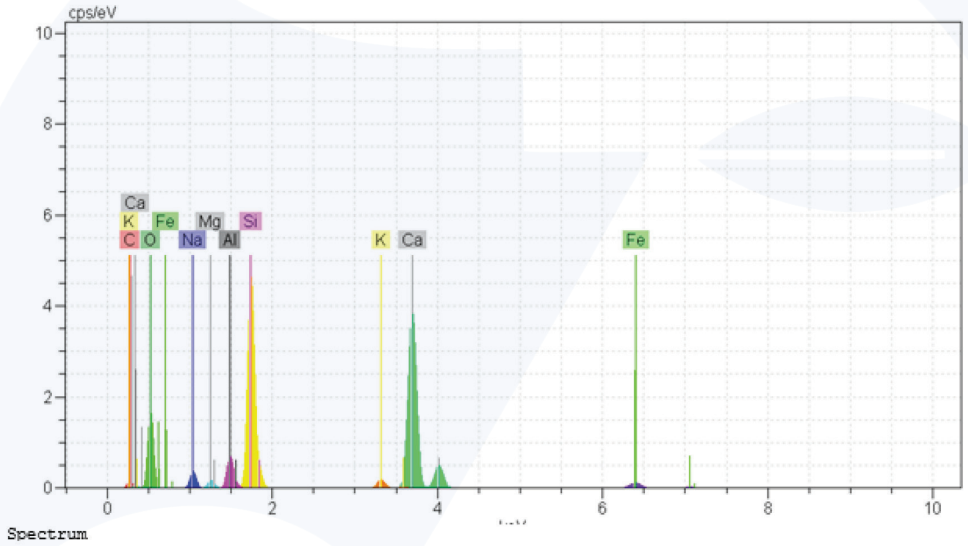

Figure 12 - Identification and abundance of the elements present in sample XI

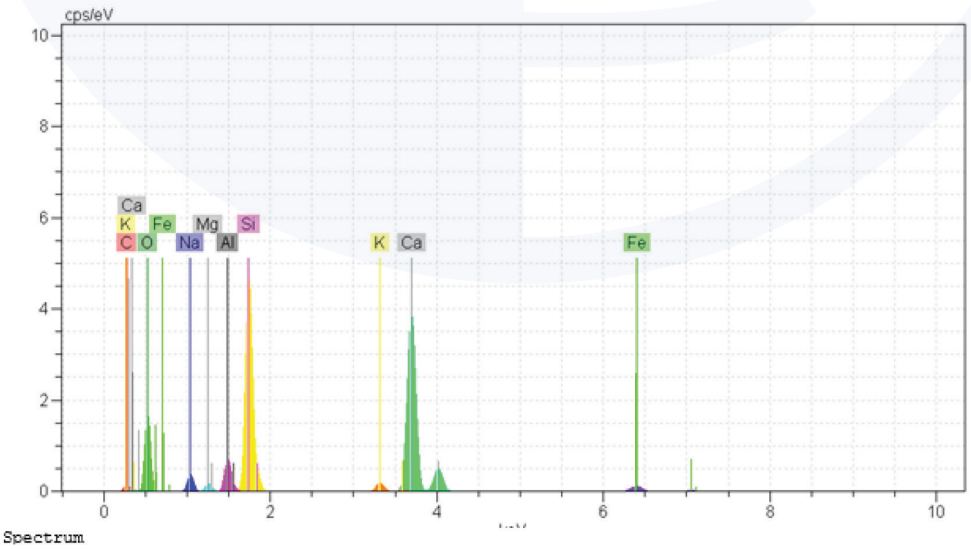

Figure 13 - Identification and abundance of the elements present in sample XII

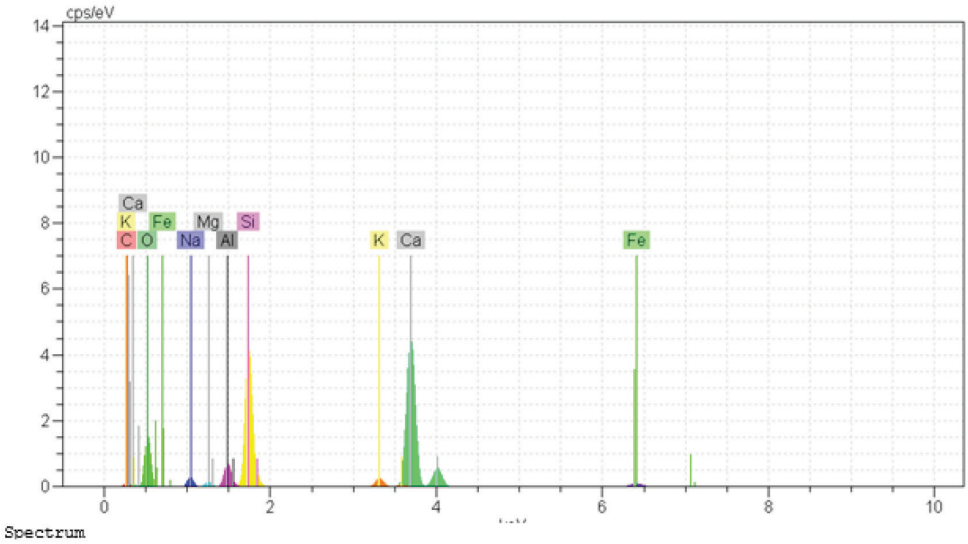

Figure 14 - Identification and abundance of the elements present in sample XIII

Table 4 . Weight percentage of the identified elements compared to the control

Name	Carbon	Oxygen	Silicon	Iron	Calcium
Control	-	-	-	-	-
TCF XI	96.77%+	13.7%-	33.5%-	86.4%+	74.9%+
TCF XII	275%+	2.3%-	31.8%-	100%+	24%+
TCF XIII	126.5%+	10.4%-	31.4%-	71.6%+	56.7%+

As mentioned earlier, silica gels begin to spread around the aggregate, usually creating a dark space around the aggregate. It can be seen in the photos that this distance is greater in the control sample. In order to ensure the qualitative analysis of SEM, which shows the intensity and amount of the identified elements, a quantitative comparison of the maximum presence of elements have been presented. Although the silica phase has a comparative priority and the gels are alkali-silica, the purposeful changes of the other elements can be considered. These can be the criteria for how the TCF(H) works.

Loss on Ignition (L.O.I)

L.O.I test was used to determine the levels of water or carbonates. The cement sample was heated to 950°C for 1.5 hours until the sample mass was stabilized. Then the amount of the lost mass was calculated.

Table 5 . Comparison of the amount of mass reduction due to combustion compared to the control

Test	XI	XII	XIII	Control
L.O.I	10.38	10.41	11.16	9.85
Percentage of the changes compared to the control	5.4%+	5.7%+	13.3%+	0---

This mass loss may indicate the presence of more materials in the samples under the TCF (H) that evaporates earlier due to heat; materials such as carbon or water from the hydration of cement or other possible materials.

XRF (X-ray fluorescence)

From each series, a sample was selected according to the maximum to minimum expansion compared to the control and the samples under the reference standard ASTM E 1621-13 and at a temperature of 21°C, the humidity of 51% based on the weight percentage of elements, and constituents by Semi-Quantitative method were analyzed by XRF.

Table 6 . Weight percentage of the oxide elements identified in the samples

Oxide	XI	XII	XIII	Control
Na_2O	2.4	2.2	2.4	2.4
MgO	1.6	1.5	1.45	1.58
Al_2O_3	7.6	7.42	7.3	8.2
SiO_2	43.7	42.5	43.2	45.5
P_2O_5	0.15	0.16	0.17	0.17
SO_3	0.48	0.57	0.54	0.42
K_2O	2.1	2.1	2.2	2.3
CaO	25.6	26.8	25.2	23.6
TiO_2	0.79	0.84	0.88	0.78
Fe_2O_3	5.2	5.5	5.5	5.2

Table 7 . Percentage of the changes of the elements compared to the control sample in XRF

Oxide	XI	XII	XIII	Control
Al_2O_3	7.13%-	9.5%-	11%-	0
SiO_2	4%-	6.6%-	5%-	0
SO_3	14.3%+	35.7%+	28.6%+	0
CaO	8.5%+	13.6%+	6.8%+	0
TiO_2	1.5%+	5.8%+	5.8%+	0

XRD (X-ray diffraction)

XRD test was taken from the samples for more accurate identification. The results of this test with respect to the general composition of cement [31-32]. are given in Table (8).

Similar to the previous test, a sample from each series was selected depending on the maximum and minimum changes compared to the control. The test was performed according to the standard BS EN 13925-1:2008 at 21°C and 51% humidity, electric current: 30 mA, voltage Kv40, anode: Cu, operating angle θ2: (10-100) degrees. Rietveld's analysis method was considered for quantitative analysis.

Step Size: 0.02, counting time: 0.5 sec

Table 8 . Identified phases in the samples under XRD

Phase	X1%	XII%	XIII%	Control%
Albite	**0.16134055**	**0.30215344**	**0.16134055**	**0.048718713**
Aluminate	6.552184	7.252681	6.552184	8.082461
Anhydrate	3.9395797	5.3288217	3.9395797	3.495407
Calcite	**11.64169**	**6.4741564**	**11.64169**	**16.603098**
Calciumsilicate	4.4278374	2.773415	4.4278374	5.016588
Dolomite	**4.7871003**	**6.83844**	**4.7871003**	**8.888318**
Ferrite	38.724575	28.624723	38.724575	29.967413
Gypsum	**2.3371325**	**15.209964**	**2.3371325**	**0.05992761**
Hemihydrate	**1.3149565**	**6.19433**	**1.3149565**	**0.08419773**
Microcline	7.396136	6.7929025	7.396136	8.271617
Periclase	12.425677	7.641237	12.425677	13.771777
Portlandite	2.3961468	2.2504933	2.3961468	2.2082295
Quartz	3.8956416	4.316682	3.8956416	3.5022485
Total	100	100	100	100

Comparison of the chemical compounds of XRD analysis

Albite contains silicon and oxygen compounds and belongs to the silicate family and has a triclinic crystal structure [33]. This compound is further developed in samples under the TCF (H).

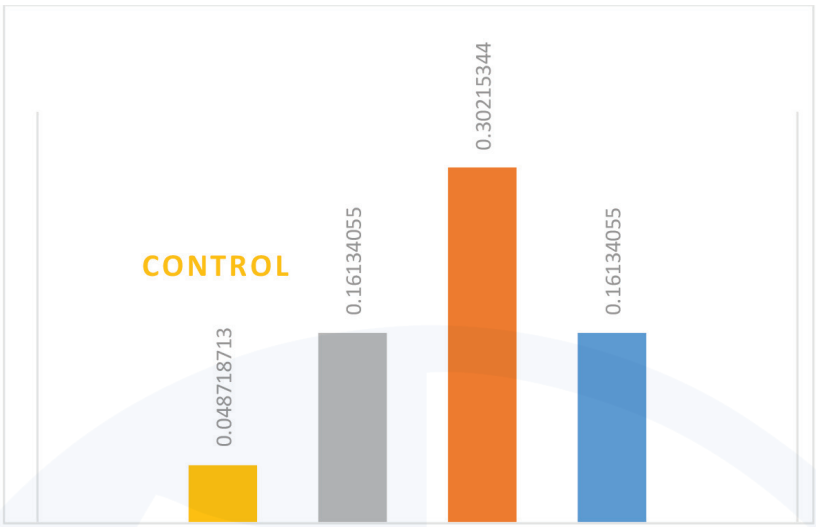

Figure 15 - Abundance of Albite in the samples

Calcite ($CaCO_3$) is a well-known form of calcium silicate. One of the parameters to which sulfates react is Ca $(OH)_2$. It is a product of cement hydration.

$Ca(OH)_2$ + cement gels (C_3S, C2S) water →+cement

Rainwater penetrates into the concrete and as it exits the capillary tubes, dissolves the Ca $(OH)_2$ created in the concrete and brings it out

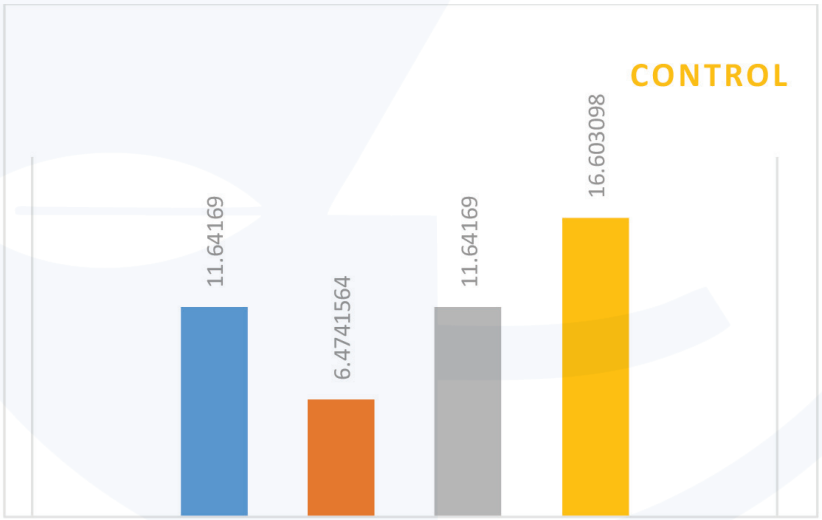

Figure 16 - Abundance of crystalline calcite in the samples

of the concrete. In the presence of air, Ca $(OH)_2$ combines with carbon dioxide and CaCO3 is formed.

After evaporation of water, $CaCO_3$ appears as white powder on the concrete surface. It also leaves a void that prepares the concrete for the sulfate's reaction. On the other hand, ambient sulfates react with $CaCO_3$ and form gypsum and aluminate gypsum compounds, which increase the volume and some specific type of sulfates reaction. In the samples under the TCF (H), we saw a sharp decrease in $CaCO_3$ [34].

Vol. 01
No. 07
April
2022
67
The First Journal in Consciousness Research

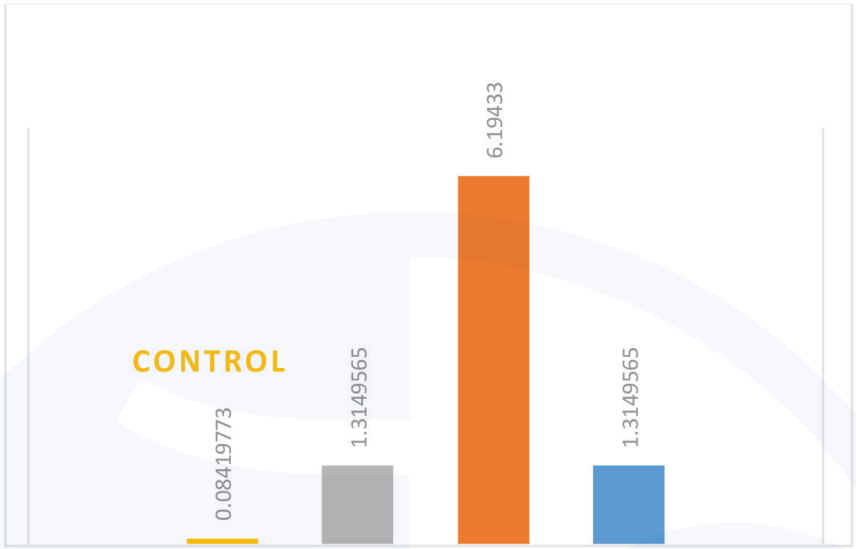

Figure 17 - Abundance of crystalline dolomite in the samples

Dolomite with the formula CaMg $(CO_3)_2$. Studies show that dolomite has a limited effect on the behavior of cement; its small amounts can improve the properties of cement and its large amounts have a reducing effect [35], And since in this process all cement has the same structure what is found after the chemical sil-ica alkali analysis is somehow the residue of the material. assuming that the amount of dolomite is the same in all samples, after the reaction, less dolomite is seen in the sample un-der the TCF (H). And dolomite on a small scale plays an alternative role to cement in increas-ing hydration.

Gypsum ($CaSO_4$. $2H_2O$) is allotropy with two molecules of calcium sulfate. In the cement industry, gypsum is used to increase the set-ting time of cement. Gypsum particles mixed with cement are very fine, forming a coating on the cement grains and preventing the rapid growth of cement crystals and instantaneous setting because the instantaneous setting is irreversible.

Sulfates attack various compounds of hydrated cement. Sodium and potassium sulfates combine with calcium hydroxide and calcium hydroaluminate. The interaction of sodium sulfate with calcium hydroxide can be summarized as follows:

$$\mathbf{Ca\ (OH)_2 + Na_2SO_4.10HO_2 \rightarrow CaSO_4.2H_2O + 2NaOH + 8H_2O}$$

And the interaction of sodium sulfate with calcium hydroaluminate is as follows:

$$\mathbf{2(3CaO.AL_2O_3.12H_2O) + (NaSO4.10H_2O) \rightarrow 3CaO.AL_2O_3.3CaSO_3.31H_2O + 2AL(OH)_3 + 6NaOH + 17H_2O}$$

One of the products of the above reactions is gypsum with the formula CaSO4·2H2O. This gypsum increases its volume and also causes resistance [2].

The chemical composition of gypsum has been seen more in the samples under the TCF (H).

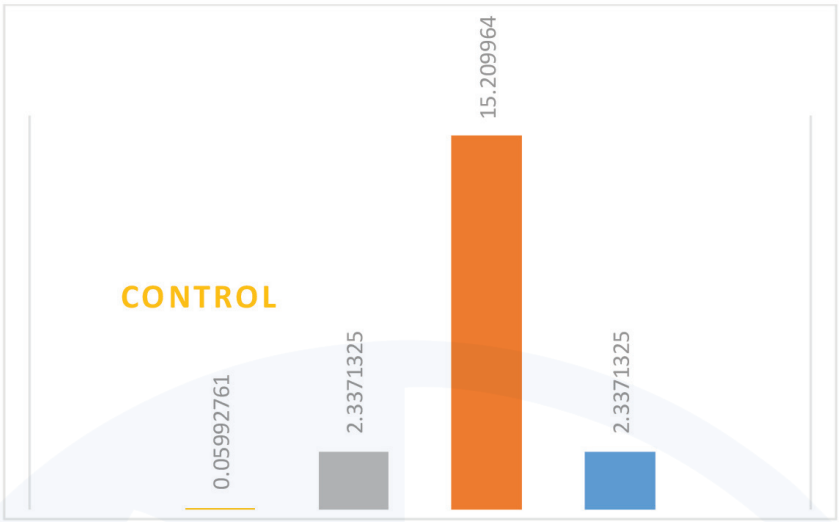

Figure 18 - Abundance of GYPSUM crystal in the samples

Hemihydrate is allotropy from calcium sulfate with the formula $CaSO_4 * 1 / 2H_2O$ and has half a unit of the water molecule. This chemical composition has been seen more in the samples under the TCF (H).

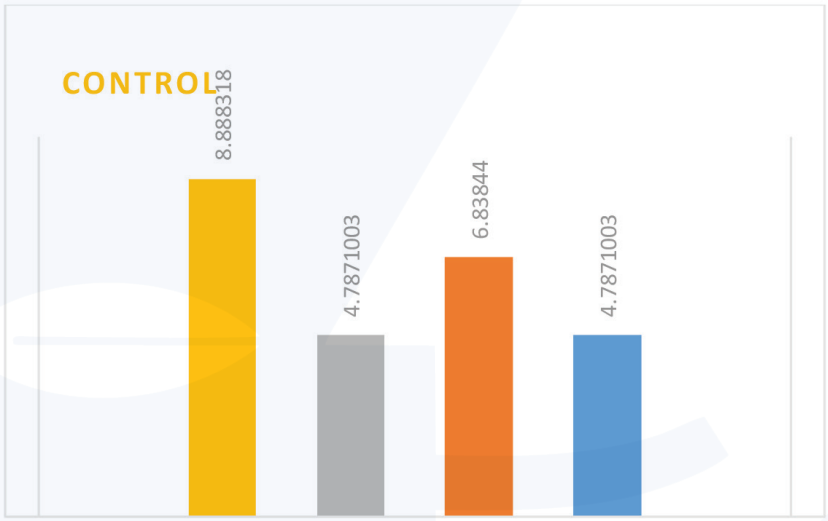

Figure 19 - Abundance of Hemihydrate crystals in the samples

The FT-IR test of infrared spectroscopy

A sample from each series was selected for FT-IR analysis. This analysis can detect vibrations in the functional groups of a sample. Existing chemical bonds stretch or bend when infrared radiation strikes the sample. Therefore, the chemical group in the sample, regardless of the structure of the rest of the molecule, tends to absorb infrared radiation in a certain range of wavelengths. As a result, based on the relationship between wavelength position and chemical structure, it is possible to easily identify different statistical groups in the sample. The position of the functional groups is almost constant. To investigate the chemical structure of the samples, the FT-IR test was used, and the results are shown in Figure 20. Also, for better comparison, the results of the magnified image of these spectra in the range of 400 cm^{-1} to 1800 cm^{-1} are also shown.

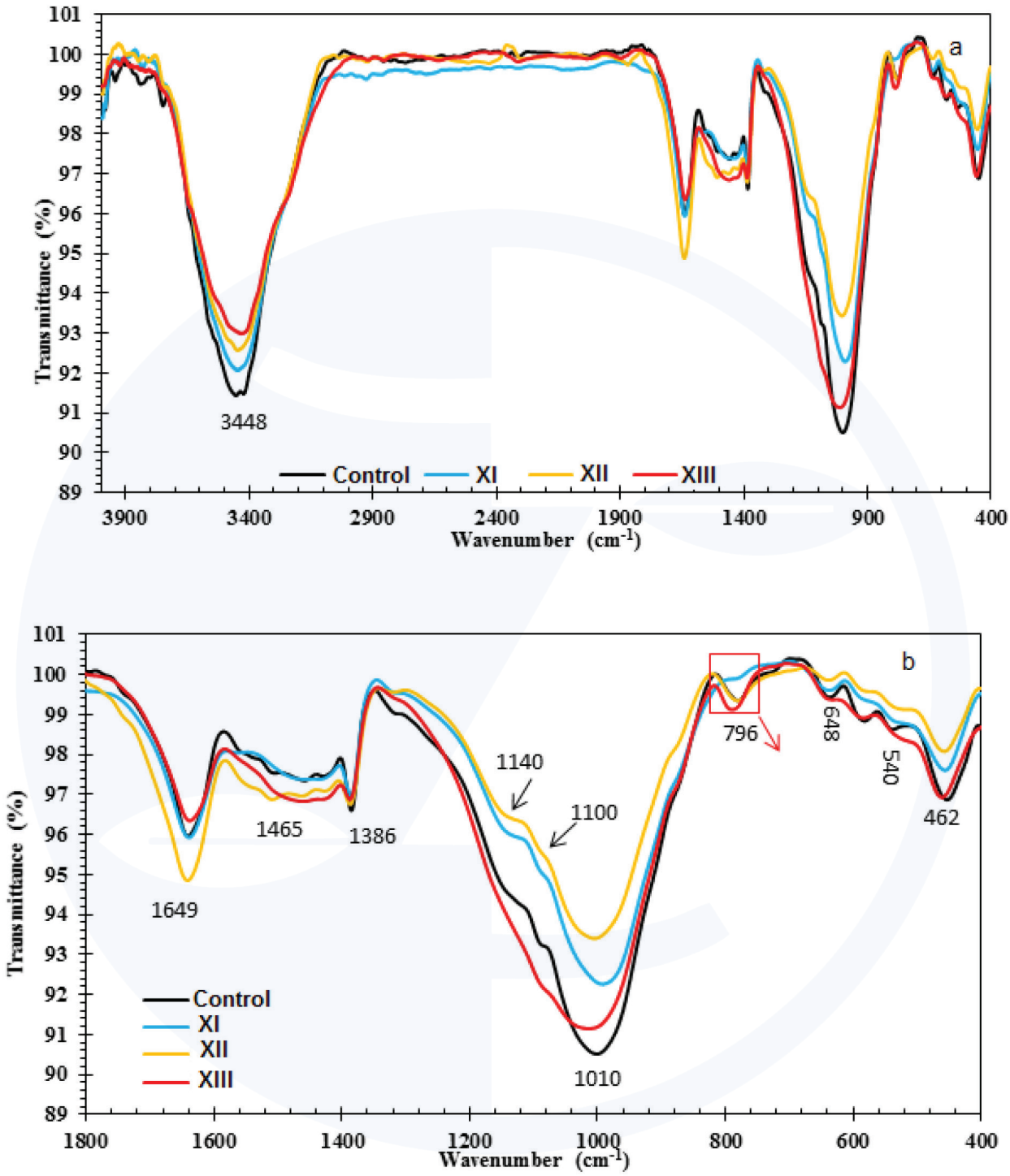

Figure 20 - Figure 20- FT-IR test results related to cement samples (a) of the whole spectrum and (b) range of 400 cm^{-1} to 1800 cm^{-1}

According to the spectra shown in Figure 20, in the studied samples, the peaks in the wave number of about 3460 cm^{-1} related to the tensile vibration of O-H bonds have been adsorbed on water molecules [36]. The same O-H bonds can vibrate at a certain frequency in the form of bending that the absorption resulting from the flexural vibration of O-H bonds has occurred in the wave number 1649 cm^{-1} [37]. The tensile vibration of the O-H bonds in the control and the flexural vibration of the O-H bonds in the samples under the TCF (H) have more pronounced peaks. Tensile vibrations of bonds in the carbonate group have shown the structure of calcium carbonate at the wave number 1465 cm^{-1}absorption peak [38]. Also, the tensile vibrations of Si-O bonds in the units of $SiO4^{-4}$ anions at the 1386 cm^{-1} wave number have shown an absorption peak [39]. The peaks appearing in the wave numbers of 1100 cm^{-1} and 1010 cm^{-1} are related to the tensile vibration of Si-O-Si and Si-O-Al bonds in the compounds present in cement, respectively [40]. This peak is seen more intensely in the control sample. The two peaks located at 648 cm^{-1}, 462 cm^{-1} and 540 cm^{-1} are also related to the flexural vibration of Si-O bonds in different compounds [40-41].

As identified in the spectrum in Figure 20, a peak is also located at wave number of 796 cm^{-1}, which is observed in samples containing high amounts of alkali in production cements. [40]. By comparing the peak intensity of this wave number, it is clear that sample XI had the lowest, and sample XIII had the highest amount of alkali in the structure. This is while the amount of alkali in control and XII were nearly identical. The amount of alkali in cement can be one of the most important parameters in cement cancer. In our experiment, the cement is the same and low-alkali and the analysis was after exposure to stimulant alkali, therefore, according to the nature of FT-IR, it can be concluded that despite the reactive medium, some amount of alkali is still seen in the XIII sample, which did not react. And this study is consistent with the results of the rate of expansion. However, according to the test conditions, the alkali of the cement must react with Normal NaOH and aggregate at the maximum state, produce an alkaline silica gel, and cause expansion. It should be noted; that this peak is usually checked to compare the alkalinity of the cement before the reaction. However, this conclusion requires an extensive review of low-alkali cement is damaging the environment.

Conclusion

In the first step, we realized that the TCF (H) was able to affect the rate of expansion of cement due to the alkaline reaction, and this effect was in the range of expansion reduction and the average of 7% (P-value0.008 -Table 3, Figure 2). According to the petrography of cement sections, it was observed that the roundness of the minerals was more noticeable in the samples under the CF(H) (Figures 3-4-5-6). Also, in SEM photography, the normal space between aggregate and cement, which is the place of gel formation, was examined. And if we examine the 10 µ scale together in the photos, in the control sample, clear crystals are seen and a larger dark space is created between the aggregate and the cement (Figures 7-8-9-10).

Elemental analysis around the aggregate clearly reveals the difference between the elements affecting this reaction (Table 4). Carbon is up to 97% higher, silicon is up to 31% lower, and iron is up to 100% higher. In the LOI test, the samples are first oxidized at 950℃ and then the mass drop is calculated. This drop is greater in the samples under the CF (H), and maybe water or carbon or materials that evaporate more easily at heat have been formed (Table 5).

Also, according to the results of the XRF analysis, there is a difference in the elements presented in Tables (6 and 7) and we see SO_3 up to 28% more and SiO2 average 5% less, CaO between 6 to 13% more, and Al_2O_3 average 9% more. The differenc-

es between the crystals seen in the XRD analysis are detailed in Table (8) and we found some compounds such as Hemihydrate, Albite, and Gypsum in the samples under the TCF (H) more and Dolomite and Calcite compounds decreased. (Figures15-16-17-18-19)

It should be noted that the way to identify phases is the possibility of the presence of elements from X-ray diffraction analysis, and since the TCF (H) has a new way of operation, what is created may not be in known formats of materials and cement. Consciousness, matter, and energy are three execution elements in our research. Therefore, we are always faced with the assumption that not all the effects of the TCF (H) can be deduced from the known custom calculations, which are limited to the laws of matter in the field of matter and energy.

These effects are more evident in the analysis of FT-IR results (Figure20). The tensile vibration of the O-H bonds in the control samples and the flexural vibration of the O-H bonds in the samples under the TCF (H) have clearer peaks. The peaks appearing in the wavenumbers of 1100 cm¯1 and 1010 cm^{-1} are related to the tensile vibration of Si-O-Si and Si-O-Al bonds in the compounds in cement, respectively, which can be seen more intense in the control sample. And in general, the difference between control graphs and the ones under the TCF (H) can be seen which has taken a different way.

As was mentioned at the beginning, the basis of the current research is to investigate the effects of TCF (H). In this theory, Although, TCFs are not measurable, it is possible to investigate their effects through various scientific research.

In this research, all the experiments have been conducted by experts unfamiliar with the theory of TCFs. Our results showed that the composition of the materials, the presence of elements, and their chemical compounds changed under the influence of TCF, and these changes were purposeful in order to control the expansion and the rate of concrete destruction. Therefore, it can be concluded that the TCF has the ability to change the behavior of materials and was able to affect favorably the process of controlling the alkaline reaction of silica by changing the chemical composition. TCF is applicable to all living (and non-living) creatures including plants, animals, microorganisms, molecules, etc. We suggest that other researchers investigate the effect of TCFs on different living and non-living creatures.

Acknowledgments

We would like to thank the international laboratories officials of Iran who patiently helped us in this research. Many thanks to Professor Ramezanianpor. Dr. Mojtahedi and Dr. Nasiri for their scientific advice and Ms. Jalayer for her work in literary and translation matters.

References

1. Mohammad. A, Ghiyasvand . E, & Nili .M. (2020). Relation between mechanical properties of concrete and alkali-silica reaction (ASR); a review. Construction and Building Materials Vol.253: 30 119189
2. Zandi .Y.(2009). Advanced Concrete Technology. ISBN:978-964-547-221-2. PP55-65
3. Kashi. M.G. (2005). Mitigation of Alkali-Silica Reactivity (ASR) for Saymareh dam Project. Soil, Rock & Structure Consulting Engineers
4. Abd-Elssamad. A, Ma. Z.J, Hou. H, Le Pape. Y. (2020). Influence of mineralogical and chemical compositions on alkali-silica-reaction of Tennessee limestones. Construction and Building Materials. Vol. 261, 20 119916
5. Stanton. T.E. (1940). Expansion of Concrete Through Reaction Between Cement and Aggregate. Proceedings of the American Society of Civil Engineers 66: 1781–1811
6. Pan. J, Feng. Y.T, Wang. J, Sun. Q.C. (2012). Modeling of alkali-silica reaction in concrete: A review. Frontiers of Structural and Civil Engineering. 6(1): 1–18 DOI 10.1007/s11709-012-0141-2
7. Lindgard. J, Andic-Caki.r O, Fernandes. I, Ronning. T. F, Thomas M D A. (2012). Alkali-silika reaction (ASR). Literature review on parameters influence laboratory performance testing, Cement and Concrete Research.Vol.42: pp.223-243
8. St John. D.A, Poole. A.B, Sims. I. (1998). Concrete Petrography-A Handbook of Investigative Techniques. Arnold, UK. pp 474.
9. Wu. H, Pan. J, Wan.g J. (2020). Nano-scale structure and mechanical properties of ASR products under saturated and dry conditions. www.nature.com/scientificreports
10. Diamond. S, et al. (1918). On the physics and chemistry of alkali-silica reaction, 5th Conf. Alkali Aggregate Reaction in concrete
11. Buck. A.D, Houston. B.J, Pepper. L. (1953). Effectiveness of mineral admixture in preventing excessive expansion of concrete due to alkali- aggregate reaction. Journal of the American Concrete Institute. Vol.30: 11-60.
12. Ramlochana. T, Thomasa. M, Grruberb. K.A. (2003). The effect of metakaolin on alkali-silica reaction in concrete. Cement and Concrete Research. Vol. 30: 339-344.
13. Rodrigue. A, Duchesne. J, Fournier. B, Champagne. M, Bissonnette.B.(2020). Alkali-silica reaction in alkali-activated combined slag and fly ash concretes: The tempering effect of fly ash on expansion and cracking. Construction and Building Materials. Vol. 251: 118968
14. Bolouri. A, Haji-Aghababayi. M. (2009). Investigation of the effect of microsilica on reducing the alkali-silica reactivity of silica in concrete aggregates of Shamil and Nian dams, First International Concrete Technology Conference, Tabriz.
15. Sedghi. P. (2009). Alkaline reaction of aggregates in concrete with a view to Gavoshan tunnel. The first national concrete conference, Tehran.
16. Singh. J, Singh. S.P.(2020). Evaluating the alkali-silica reaction in alkali-activated copper slag mortars. Construction and Building Materials. Vol. 253: 119-189
17. Delnavaz. M, Family. H, Khaksari. M, Alipour. B.(2010). Investigating the effect of using nano-silica, silica fume and metakaolin on reducing alkali-silica reactions of concrete aggregates, 2nd National Concrete Conference Tehran-Iran . https://civilica.com/doc/152568
18. Feng. X, Thomas. M.D.A, Bremner. T.W, Balcom. B.J, Folliard K. J. (12005). Studies on lithium salt to mitigate ASR-induced expansion in new concrete: a critical review, Cement and Concrete research. Vol.35: 1789-1796
19. Kim. T, Olek. J. (2016). The effects of lithium ions on chemical sequence of alkali-silica reaction. Cement and Concrete Research. 79: 159-168.
20. Afshinnia. K, Poursaee. A. (2015). The influence of waste crumb rubber in reducing the alkali-silica reaction in mortar bars. Journal of Building Engineering. 4: 231-236
21. Le .H.T, Ludwig. H. M. (2020). Alkali silica reactivity of rice husk ash in cement paste. Construction and Building Materials Vol. 243: 118145.
22. Ahmadi. B, Shekarchi .M. (2010).Use of natural zeolite as a supplementary cementitious material. Cement and concrete composites. Vol.32 (2) pp134-141
23. Najmi. M, Sobhani. J, Ahmadi. B, Shekarchi. M.(2012). An experimental study on durability properties of concrete containing zeolite as a highly reactive natural pozzolan. Construction and Building Material. Vol. 35: pp 1023-1033.
24. Snyder. K. A, Lew. H. S. (2013). Alkali-Silica Reaction Degradation of Nuclear Power Plant Concrete Structures: A Scoping Study. Materials and Structural Systems Division Engineering Laboratory. NISTIR 7937
25. WWW.cosmointel.com
26. Taheri. .M. A. (2013). Human from another outlook. Interuniversal Press. 2nd Edition. ISBN-13: 978-1939507006, ISBN-10: 193950700
27. Taheri. M.A. (2012). General Connection of particles. Interuniversal Publishing.Erfan-Hlgheh. ID: 978-1-940491-03-5
28. Torabi.S., Taheri. M. A., & Semsarha, F. (2020). Alleviative effects of Faradarmani Consciousness Field on Triticum aestivum L. under salinity stress. F1000Research, 9(1089), 1089.
29. Astm. ASTM C1260-Standard test method for potential alkali reactivity of aggregates (mortar-bar method). ASTM Int. 2012. 1-5.
30. Esfahani. A.N, Ahmadi.M,(2005). Petrography of igneous rocks, Islamic Azad University. (Khorasgan). ISBN:964-95173-7-5
31. Stutzman. P, Feng. P, Bullard . J. (2016). Phase Analysis of Portland Cement by Combined Quntitative X-Ray Powder Diffraction and Scanning Electron Microscopy. Journal of Research of the National Institute of Standards and Technology. Vol. 121 http://dx.doi.org/10.6028/jres.121.004,
32. Le Saoût. G, Kocaba. V, Scrivener. K. (2011). Application of the Rietveld method to the analysis of anhydrous cement. Cement and Concrete Research. 41 133–148
33. Khodam. F. (2018). X Ray Diffraction (XRD) Spectroscopy. NAIS. vol. 2: pp 11-19. Print ISSN: 2588-6401., Online ISSN: 2588-641X
34. Zandi. Y.(2009). Advanced Concrete Technology. ISBN:978-964-547-221-2.,PP 2-10
35. Sybilskia. M, Nocun-Wczelikb. W, Gorazdze. C. (2015). The effect of dolomite additive on cement hydration. Peer-review under responsibility of organizing committee of the 7th Scientific-Technical Conference Material Problems in Civil Engineering. DOI 10.1016/j.proeng.06.136
36. Javidparvar. A.A, Ramezanzadeh .B, Ghasemi. E. (2016). The effect of surface morphology and treatment of Fe3O4 nanoparticles on the corrosion resistance of epoxy coating, J. Taiwan Inst. Chem. Eng. 61. https://doi.org/10.1016/j.jtice.2016.01.001
37. Anchieta .C, Cancelier. A, Mazutti. M, Jahn .S, Kuhn .R, Gündel .A, Chiavone-Filho .O, Foletto E.(2014). Effects of Solvent Diols on the Synthesis of ZnFe2O4 Particles and Their Use as Heterogeneous Photo-Fenton Catalysts, Materials (Basel). 7 (2014) 6281–6290. https://doi.org/10.3390/ma7096281.
38. Sasnauskas. V. (2013). Cement hydration with zeolite-based additive, Chemija. 24 -271–278.
39. Hassan. M, J. M. Khatib, P. S. Mangat, and P. H. E. Gardiner. (2014). "FTIR and XRD Characterized Portland Cement Stabilised Lead Contaminated Soil." .
40. Tyler. S. (2001). Application of FTIR for Quantification of Alkali in Cement. The University of North Texas.
41. Trezza M. A. (2007). Hydration study of ordinary portland cement in the presence of zinc ions. Materials research. Dec;10(4):331-4.